Optical and Quantum Electronics **15** *(1983) 381–388*

Combined reciprocal and non-reciprocal birefringence in optical monomode fibres

VALERIO ANNOVAZZI-LODI, SILVANO DONATI
Istituto di Elettronica e Comunicazioni Elettriche, Università di Pavia, Strada Nuova 106/c, Pavia, Italy

Received 15 November 1982

We analyse the overall birefringence which arises from the combined effects of Faraday rotation (non-reciprocal) and bending stress (reciprocal) applied to a monomode optical fibre loop. The theory is substantiated by numerical evaluations and appropriate experimental data are reported. These indicate how it is possible to build non-reciprocal birefringent components, i.e. rotators and isolators, by means of monomode coils.

1. Introduction

In addition to the applications in telecommunication systems, monomode optical fibres have been considered in instrumentation as candidates for a number of sensors (pressure, mechanical strains, magnetic fields and current intensity) [1, 2]. In these devices, one exploits the effects of induced birefringence, which can be measured with high sensitivity through interferometric methods, thus allowing the construction of a so-called monomode sensor.

Recently, it has been demonstrated that birefringent components can be built using short pieces of monomode fibre to which a controlled external stress or bending [3–5] is applied, and these components have been used in the fibre gyroscope, where they allow the integration of the phase-modulator and couplers in the fibre medium.

In a previous paper [3], we presented the analysis of fibre-optic reciprocal devices. In this work, we take into account the combination of the Faraday rotation due to a magnetic field applied to the fibre, and of the linear birefringence either residual or externally introduced through the fibre bending. The case of bending, the one of a fibre coil, is interesting from the application point of view because it allows one to build an optical isolator or a magnetic field sensor which is far more compact than the straight-fibre version previously proposed [6].

An analysis of Faraday rotation in a fibre loop for one special case has been reported by Day *et al.* [7]. We develop the approach further by treating the general case of superposition of Faraday and linear birefringence effects in a monomode fibre for all states of polarization and launch conditions.

2. Theoretical analysis

2.1. General analysis

It is well known [8] that by applying a magnetic field **H** to a fibre sample L of negligible birefringence, a non-reciprocal rotation of the polarization direction is induced, and the rotation angle F between output and input is given by

$$F = V\int_L \mathbf{H}\cdot\mathbf{dl} \tag{1}$$

where V is the Verdet constant of the material.

If both uniform linear birefringence and uniform Faraday rotation are present, their superposition can be expressed in terms of a Jones matrix [8–11], i.e.

0306–8919/83 $03.00 + .12

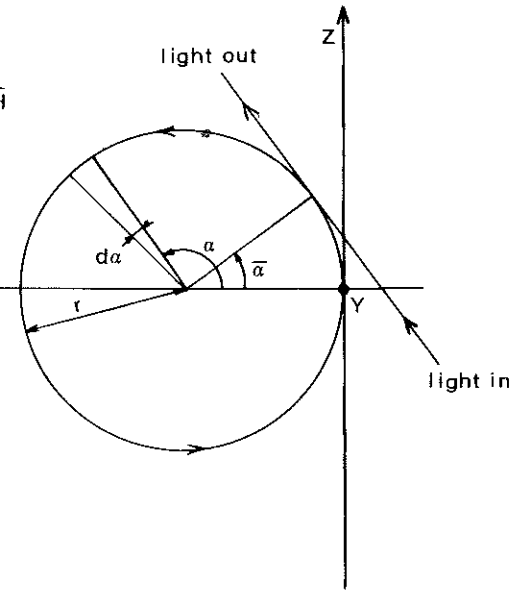

Figure 1 Fibre loop in a magnetic field: the arrows show the direction of propagation of the injected light.

$$\begin{bmatrix} E_x \\ E_y \end{bmatrix}_z = \begin{bmatrix} A & -B \\ B & A^* \end{bmatrix} \begin{bmatrix} E_x \\ E_y \end{bmatrix}_0 . \tag{2}$$

e E_x and E_y are the complex amplitudes of the electric field, and the matrix elements A and B can be ten as

$$\begin{aligned} A &= \cos\phi/2 + j\cos\chi\sin\phi/2 \\ B &= \sin\chi\sin(\phi/2) \end{aligned} \tag{3}$$

re ϕ and χ are combinations of the total Faraday rotation F and linear birefringence phase delay δ, ch read [8]:

$$\begin{aligned} (\phi/2)^2 &= (\delta/2)^2 + F^2 \\ \tan\chi &= F/(\delta/2). \end{aligned}$$

n a fibre loop of radius r, as in Fig. 1, the linear birefringence induced by bending is uniform and its e shift is proportional to $(\alpha - \bar{\alpha})/r$ [3]; by contrast, the Faraday rotation due to a uniform magnetic H applied to the loop has a sine-dependence, i.e.

$$F(\alpha) = V\int_{\alpha}^{\bar{\alpha}} Hr\cos\alpha\,d\alpha = VHr(\sin\bar{\alpha} - \sin\alpha). \tag{4}$$

similar kind of interaction between birefringence effects [6] arises in a straight fibre of high nsic linear birefringence placed in a sine-wave modulated magnetic field changing its sign over a od l. It has been shown [6] that the overall Faraday rotation on a long piece of fibre is very small pt when l is just equal to the beating length of the birefringent fibre. Correspondingly, we may ct as a condition for a net Faraday rotation that the loop should be a 2π retarder [7]. This gives a ite value of the bending radius r [3] required to enhance the non-reciprocal effect.

o start our analysis, let us characterize the state of polarization along the fibre with the complex R defined as

$$R = \frac{E_x}{E_y} = |R|\,e^{i\theta} \tag{5}$$

he evolution of R can be assumed as a complete description of the birefringence effects [12], pro-

vided the bending attenuation is negligible. Since Equation 2 holds only for a uniform Faraday rotation, we may apply it to a small piece dl of the fibre loop (see Fig. 1), for which:

$$\begin{aligned} \mathrm{d}F &= V H r \cos\alpha \, \mathrm{d}\alpha \\ \mathrm{d}\delta &= c\, r \, \mathrm{d}\alpha \\ c &= \delta/2\pi r \end{aligned}$$

Here, H is the field component in the plane of the fibre loop.

The Jones matrix for dl then becomes, for $F \ll \delta$:

$$[T] = \begin{bmatrix} 1 & 0 \\ 0 & 1 \end{bmatrix} + \begin{bmatrix} \mathrm{d}A & -\mathrm{d}B \\ \mathrm{d}B & \mathrm{d}A^* \end{bmatrix}$$

where the infinitesimal elements dA and dB can be found by substitution in Equation 2 as:

$$\begin{aligned} \mathrm{d}A &= j\left(\frac{cr}{2} + \frac{(VH)^2}{c} r \cos^2\alpha\right) \cos\left(2\frac{VH}{c}\cos\alpha\right) \mathrm{d}\alpha \\ \mathrm{d}B &= \left(\frac{cr}{2} + \frac{(VH)^2}{c} r \cos^2\alpha\right) \sin\left(2\frac{VH}{c}\cos\alpha\right) \mathrm{d}\alpha \end{aligned} \tag{6}$$

while for the ratio R we obtain:

$$\mathrm{d}R = (\mathrm{d}A - \mathrm{d}A^*)R - (1 + R^2)\,\mathrm{d}B. \tag{7}$$

A Riccati's differential equation then arises for R:

$$R'(\alpha) = 2jM(\alpha)\cos K(\alpha)\, R - M(\alpha)\sin K(\alpha)\, R^2 - M(\alpha)\sin K(\alpha) \tag{8}$$

where

$$M(\alpha) = \frac{cr}{2} + \frac{(VH)^2}{c} r \cos^2\alpha \tag{9}$$

$$K(\alpha) = 2\frac{VH}{c}\cos\alpha \qquad c = \delta/2\pi r. \tag{10}$$

Equation 8 describes the state of polarization at any point of the loop, provided that we specify the input state:

$$R(\bar{\alpha}) = \left.\frac{E_x}{E_y}\right|_{\alpha=\bar{\alpha}}$$

Here, $\bar{\alpha}$ is the input angle on the loop, i.e. the angle between the magnetic field vector **H** and the light wave vector at the injection point. In the above we require that R is a finite quantity over the whole range of integration. If the condition $|R| < \infty$ is not satisfied, but $R \neq 0$ holds over the whole sample, we can use Equation 8 simply by interchanging x and y (i.e. R and $1/R$), and changing the sign of α.

The Riccati Equation 8 does not admit of a general analytical solution, and below we consider the special cases of interest.

2.2. Special cases

Let us now consider an input field linearly polarized along the y-axis and a weak magnetic field H so that $|R| \ll 1$ all over the loop; this is the most frequent case, e.g. when working with H up to about 4×10^6 Am^{-1} (50 kOe) for silica fibres. Then Equation 8 can be linearized, i.e.

$$R'(\alpha) = 2j\left(\frac{cr}{2} + \frac{(VH)^2}{c} r\cos^2\alpha\right)R - 2\left(\frac{cr}{2} + \frac{(VH)^2}{c} r\cos^2\alpha\right)\frac{VH}{c}\cos\alpha \tag{11}$$

and it is integrated easily with the following result, valid for $F \ll \delta$:

$$R(\alpha) = -VHr\, e^{jcr\alpha}\int_{\bar{\alpha}}^{\alpha} e^{-jcr\alpha}\cos\alpha\, d\alpha + e^{jcr(\alpha-\bar{\alpha})}R(\bar{\alpha}) \tag{12}$$

If $c = 1/r$ (i.e. the fibre loop behaves as a linear 2π-retarder when the magnetic field is removed) we finally obtain

$$R(\alpha) = -\frac{HVr}{2} e^{j\alpha}[(\alpha-\bar{\alpha}) + \tfrac{1}{2}(\sin 2\alpha - \sin 2\bar{\alpha}) + \tfrac{1}{2}j(\cos 2\alpha - \cos 2\bar{\alpha})] + R(\bar{\alpha})\, e^{j(\alpha-\bar{\alpha})}. \tag{13}$$

This equation shows that for an input at $\bar{\alpha} = 0$ with a linearly y-polarized state, i.e. $R(0) = 0$, the output state after one turn will be still linearly polarized, i.e. Im $[R(2\pi)] = 0$, but the polarization direction has been rotated, as expected. The rotation amounts to:

$$\Delta\phi_R = \arctan(-VHr\pi)$$

and since for silica $V = 4.83 \times 10^{-4}$ rad/(Oe m) the following approximation applies for all practical H intensities:

$$\Delta\phi_R \cong -VHr\pi \tag{14}$$

in accordance with the result reported by Day *et al.* [7]. The negative sign corresponds to a clockwise rotation, according to Fig. 1 and to the definition of R.

In spite of the restriction $|R| \ll 1$ by which it was derived, Equation 14 represents a quite general result, because it will be shown, both through numerical evaluations and experimentally, that also for a general state of polarization injected at $\bar{\alpha} = 0$, the overall birefringence effect consists of a pure rotation of the principal axes, $\Delta\phi_R$ being expressed by Equation 14.

When $\bar{\alpha} = 0$, one can see from Fig. 1 that reversing the direction of propagation is equivalent to reversing the sign of H. We can therefore conclude from Equation 14 that the rotation effect just described is non-reciprocal; this has been confirmed both experimentally and numerically (from Equation 8) for any input polarization (see Section 3).

A pure, polarization independent non-reciprocal rotation can therefore be obtained using 2π loops and entering at $\bar{\alpha} = 0$. Obviously, the rotation angle can be increased simply by cascading many loops, i.e. making a coil.

For different orientations of the vector **H** (i.e. for an input at a different point $\bar{\alpha}$), as well as for different values of r, there will be a superposition of reciprocal and non-reciprocal birefringence and the emerging field will be in general elliptically polarized. As an example, consider $\bar{\alpha} = \pi/2$; for a y-linearly polarized input field Equation 13 predicts, after one turn, an elliptical output state, but no rotation of axes, i.e. $\mathrm{Re}[R(2\pi)] = 0$; the ellipticity angle $\Delta\phi_E$ defined as:

$$\Delta\phi_E = \arctan(b/a)$$

where a and b are the elliptical polarization principal axes, amounts to:

$$\Delta\phi_E \cong -VHr\pi. \tag{15}$$

This effect can be easily shown to be fully reciprocal.

The special case $R \cong 1$ can be treated by making the substitution $R = 1 + P$ $(P \ll 1)$ in Equation 8, while the case $|R| \to \infty$ can be reduced as shown at the end of Section 2.1. For injection at the point $\bar{\alpha} = 0$, Equation 14 still holds, confirming for the present cases the independence of the Faraday effect from the input polarization. For $\bar{\alpha} = \pi/2$ Equation 15 also gives the correct result.

Moreover, from Equation 13 it is seen that, if $R(\bar{\alpha}) = 0$:

$$R(\bar{\alpha} + 2\pi) = -VHr\pi(\cos\bar{\alpha} + j\sin\bar{\alpha})$$

i.e. V, H and r are scale factors only, and the dependence of Re (R) and Im (R) on the input angle $\bar{\alpha}$ has a sinusoidal form. If $VHr\pi \ll 1$, it can be shown that

$$\begin{aligned}\Delta\phi_R &\cong -VHr\pi\cos\bar{\alpha}\\ \Delta\phi_E &\cong -VHr\pi\sin\bar{\alpha}.\end{aligned} \tag{16}$$

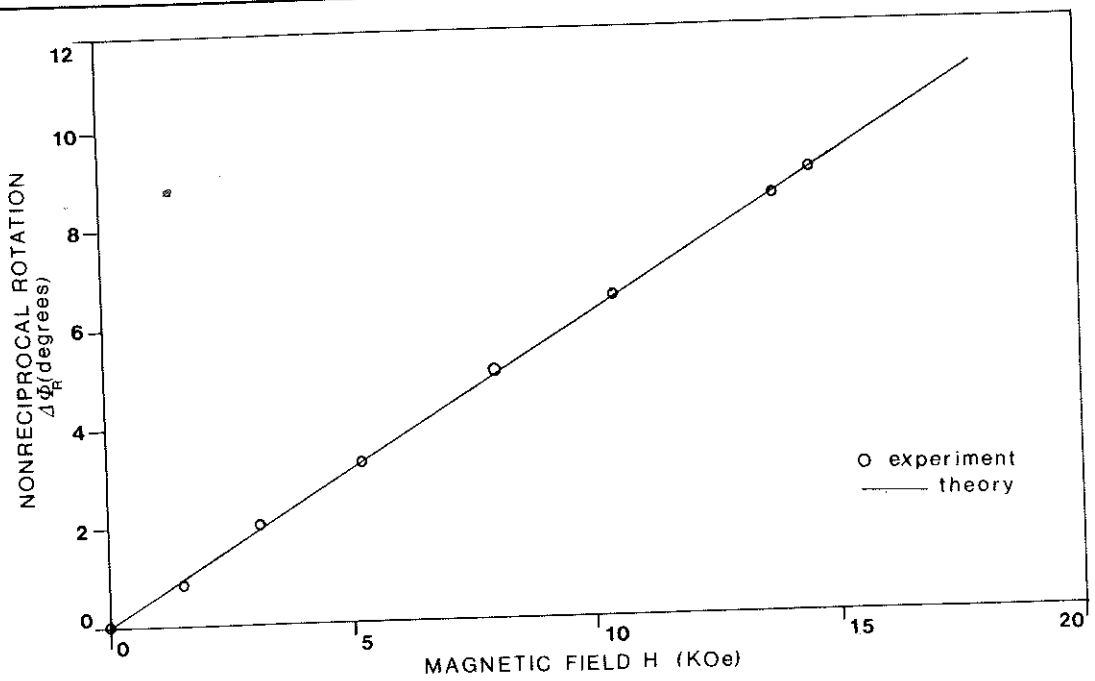

Figure 2 Non-reciprocal Faraday rotation as a function of H, for a 2π-delay loop.

Finally, an examination of Equation 8 for $c = n \cdot 1/r$ ($n = 2, 3 \ldots$), shows that no overall birefringence effect takes place for any input polarization and H-field orientation, i.e. the $2n\pi$ loop simply behaves as a λ-retarder. By contrast, for all other values of c, a non-zero effect is found. This circumstance is of interest in minimizing the effects of environmental magnetic fields on a coil, e.g. in a fibre gyroscope.

3. Experimental results and numerical analysis

In order to test Equations 8 and 13, experiments were made on a sample of small-residual-birefringence monomode fibre supplied by Valtec (SM05). The source was a single mode 5 mW He–Ne laser; both an electromagnet ($H \leqslant 1.6 \times 10^6$ A m^{-1} (20 kOe)) and permanent magnets ($H \sim 1.27 \times 10^5$ A m^{-1} (1.6 kOe)) were used. In addition, numerical analysis was performed by decomposition of Equation 8 into a system of two real-coefficient differential equations and integration through a fourth-order Runge–Kutta routine.

These evaluations show that Equation 8 represents an adequate description of the Faraday effect in the general case, while Equation 13 correctly describes the important case $\bar{\alpha} = 0$ for any input state of polarization. In the following, we report the main experimental and numerical results pertinent to cases of practical interest.

3.1. Experiments

Fig. 2 shows the non-reciprocal rotation angle $\Delta\phi_R$ as a function of the transverse magnetic field H for a single loop. The correct bending radius ($r \cong 5.5$ mm) was evaluated from the expression reported in [3]; a fine trimming ensured a correct 2π-delay. The points shown in the diagram represent the maximum observed rotation angle which, within a small error, differing from sample to sample, was however found to be in correspondence with the expected value of the angular coordinate (i.e. $\bar{\alpha} = 0$).

As can be seen, experimental results agree satisfactorily with the theoretical ones given by Equations 14, represented by the straight line on the diagram ($V = 3.4 \times 10^{-4}$ degrees A^{-1} (2.76×10^{-2} degrees

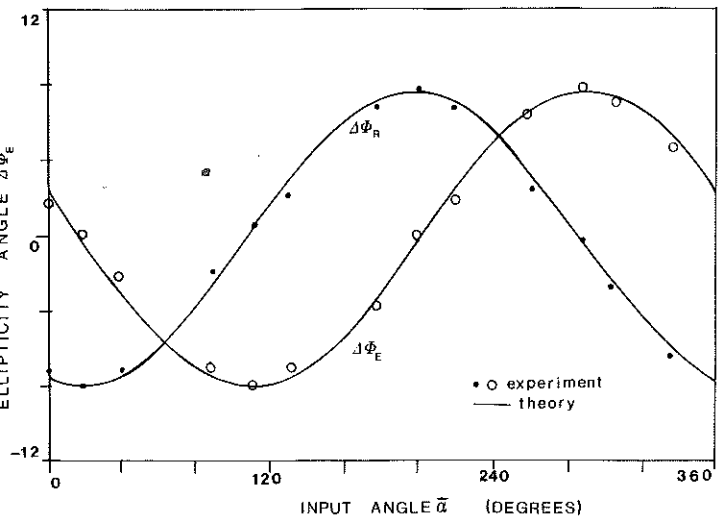

Figure 3 Non-reciprocal Faraday rotation $\Delta\phi_E$ and ellipticity angle $\Delta\phi_E$ as a function of $\bar{\alpha}$, for a y-linearly polarized field injected into a coil of ten 2π-delay loops.

$^{-1}\,m^{-1}$). As anticipated previously, it was found experimentally that the rotation does not depend on injected state of polarization, if $\bar{\alpha} = 0$. Also, the non-reciprocity of this effect was carefully checked. Fig. 3 shows the rotation angle $\Delta\phi_R$ and the ellipticity angle $\Delta\phi_E$ for a linear polarization ($R(\bar{\alpha}) = 0$) ering a coil of ten 2π-loops as a function of the input angle (or of the orientation of the vector **H**). e fibre was put into the gap of an AlNiCo III permament magnet giving a field of 1.27×10^5 A m^{-1} 00 Oe). Though the general trend was well verified, an input angle shift was necessary in order to ain an accurate fit to the theoretical curves (Equation 16); the shift varied with the sample and eared attributable to residual fibre birefringence and launching effects.

When assembling a coil it was found better to trim each loop to maximize the non-reciprocal effect. ractice, small errors can be tolerated if they cancel out over the whole coil; however, doing so, we nd that the direction of H giving the maximum rotation can differ appreciably from the expected e ($\bar{\alpha} = 0$).

2. Numerical analysis

e dependence of $\Delta\phi_R$ and $\Delta\phi_E$ on the input polarization was evaluated numerically for different ues of the input angle $\bar{\alpha}$, using Equation 8. In the following we summarize these results, with erence to a 2π-loop. For $\bar{\alpha} = 0, \delta = 2\pi$, we found, as expected, a pure non-reciprocal rotation. Using same values for the parameters as in our own experimental arrangement, i.e. $H = 1.27 \times 10^5$ A m^{-1} 00 Oe) and $r = 5.5$ mm, we obtained $\Delta\phi_R = -0.79°$, $\Delta\phi_E = 0$ (within a small error) for any linear, ular or elliptical input polarization. In these conditions, parameters r and H were confirmed to be y scale factors. Fig. 4 shows the evolution of $\Delta\phi_R$ and $\Delta\phi_E$ on a whole 2π-loop for $\bar{\alpha} = 0, R(0) = 0$, $= 1.27 \times 10^5$ A m^{-1} (1600 Oe), $r = 5.5$ mm, $V = 3.4 \times 10^{-4}$ degrees A^{-1} (2.76×10^{-2} degrees $^{-1}$ m^{-1}).

In the general case $\bar{\alpha} \neq 0$ the birefringence effect is more complex. For $\bar{\alpha} = \pi/2$ and the above orted values of the other parameters, we found $\Delta\phi_E = -0.79°$, $\Delta\phi_R = 0$ for any input polarization ose principal axes are x and y. For $\bar{\alpha} = \pi/4, R(\pi/4) = 0$, we found $\Delta\phi_R = -0.59°$, $\Delta\phi_E = -0.56°$, $\Delta\phi_E \cong \Delta\phi_R$.

Finally, the dependence on δ was investigated; we found that small deviations from the nominal ue $\delta = 2\pi$ can result in a large cumulative error in the operation of a birefringent component, as wn below. The general dependence of the birefringent effect on δ was however found to be rather nplicated.

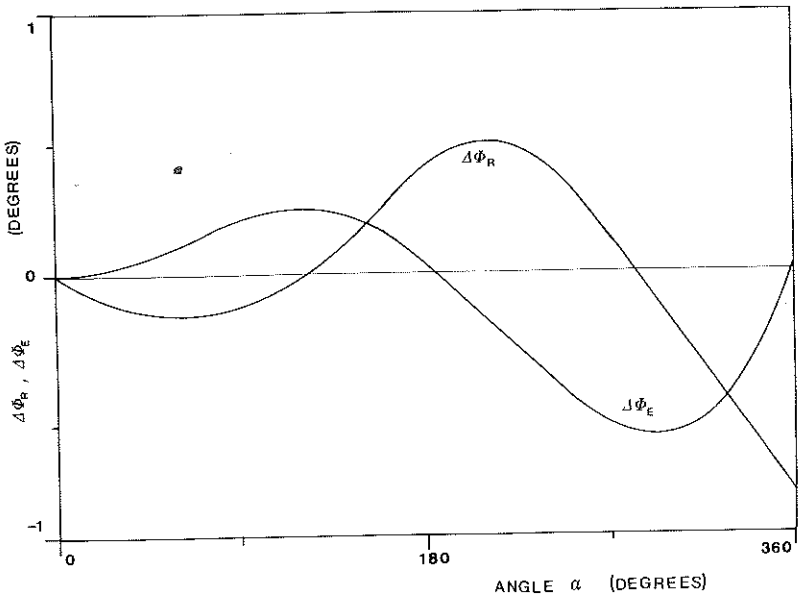

Figure 4 Evolution of $\Delta\phi_R$, $\Delta\phi_E$ through a whole 2π-delay loop for $R(0) = 0$ and for typical values of parameters (see text).

3.3. Applications

From the preceding results, it is evident that there is a possibility of building an optical isolator. This component is useful for matching single mode injection lasers to fibre pigtails because it has been found that back-reflections and back scattering perturb the active component both in frequency and amplitude [13] so offsetting the advantage of single mode fibre for optical communication applications. The isolator, with an almost unity transparency in one direction and a strong attenuation in the opposite direction, solves this problem (provided its own back scattering is low).

If SmCo magnets are used, the number of turns will be relatively small and the bending attenuation will be compatible with most applications [3]. For example to obtain a 90° non-reciprocal rotation difference in the two-way propagation one can use a 5.5 mm radius coil with $B = 1.21 \times 10^6$ A m^{-1} (15.2 kOe) and $N = 6$ turns of Valtec SM05. This component must be built with a small mechanical tolerance on the bending radius r to ensure a correct operation. For example, an error $\Delta r = 0.3$ mm, gives, after four turns, $\Delta\phi_R = -21°$, $\Delta\phi_E = 26°$ while the expected values for $r = 5.5$ mm ($\delta = 2\pi$) are $\Delta\phi_R = -30°$, $\Delta\phi_E = 0$.

Moreover, the coil described above finds an obvious application as a sensor for magnetic fields. In particular it gives the starting point for a passive, isolated current sensor. Note that in this approach it is not required to pass the conductor inside [14] the fibre coil. To develop the approach further, we have built a sensor with the geometry reported in Fig. 5 so as to improve responsitivity. The coil was made by 12 loops of 2π phase-shift. The fibre was fed by a He–Ne source and the output state was detected by a polarizer and a photodiode. Fig. 5 shows the output voltage from the photodiode as a function of the amplitude of an a.c. current (50 Hz) fed into a conductor at about 5 cm from the coil. By proper design it seems quite easy to reach a sensitivity in the ampere range, useful for current measuring in high and medium voltage distribution lines.

Finally, the above theory allows one to evaluate the error due to environmental magnetic fields in the inertial rotation measurement performed by a fibre gyroscope. The importance of this contribution appears evident if we consider that the earth magnetic field would give a $\Delta\phi_R$ of about 200 μrad s^{-1} for a 100 m fibre sample and a coil radius of 30 cm when each loop is a λ-shifter. This result, in agreement with that reported in [15], is well in the range of sensitivity of the present gyroscopes, confirming that magnetic immunity has to be evaluated in an actual device by taking into account both residual and stress-induced birefringence.

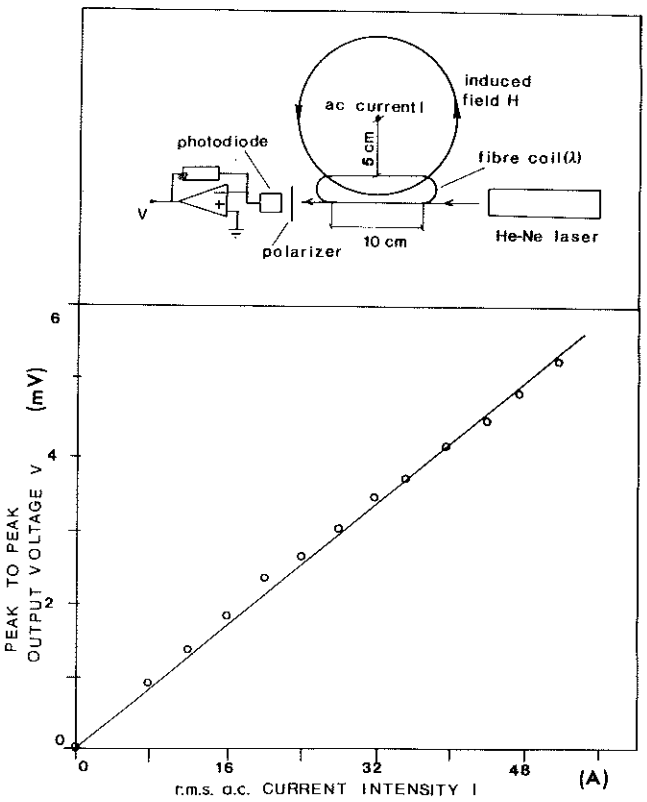

Figure 5 Experimental evaluation of a fibre-optic sensor for a.c. currents, see text.

Acknowledgements

This work was supported by the "Consiglio Nazionale delle Ricerche". One of us (VAL) performed this work under a fellowship awarded by Selenia Industrie Elettroniche Riunite SpA, Roma.

References

1. D. McMAHON, A. NELSON and W. SPILLMAN, *IEEE Spectrum* **12** (1981) 24–9.
2. C. LIGUORI and M. MARTINELLI, *Appl. Opt.* **20** (1981) 4319–23.
3. V. ANNOVAZZI-LODI and S. DONATI, *Alta Frequenza* **3** (1982) 159–63.
4. R. ULRICH and A. SIMON, *Appl. Opt.* **18** (1979) 2241.
5. R. ULRICH, S. C. RASHLEIGH and W. EICHOFF, *Opt. Lett.* **5** (1980) 273.
6. R. M. STOLEN and E. M. TURNER, *Appl. Opt.* **19** (1980) 842.
7. G. W. DAY, D. N. PAYNE, A. J. BARLOW and J. J. RAMSKOV-HANSEN, *Opt. Lett.* **7** (1982) 238–40.
8. A. M. SMITH, *Appl. Opt.* **17** (1980) 52.
9. R. C. JONES *JOSA* **31** (1941) 488.
10. W. J. TABOR and F. S. CHEN, *J. Appl. Phys.* **40** (1968) 2760.
11. G. FRANCESCHETTI and C. PORTER-SMITH, *JOSA* **71** (1981) 1487–91.
12. M. BORN and E. WOLF, 'Principles of Optics' (Pergamon Press, New York, 1975) pp. 24–6.
13. V. ANNOVAZZI-LODI and S. DONATI, *J. Quant. Elect.* **QE 16** (1980) 859.
14. A. PAPP and H. HARMS, *Appl. Opt.* **19** (1980) 3729.
15. K. BÖHM, K. PETERMANN and E. WERDEL, *Opt. Lett.* **7** (1982) 180.